Matching-network boosting enabling reconfigurable pMUTs for IoT sensor node applications

Gabriel Giribaldi*, Bernard Herrera Soukup*, Pietro Simeoni *, Luca Colombo*, Matteo Rinaldi*
*SMART Center, Northeastern University, Boston MA, USA

Abstract—This paper presents an architectural technique to improve the performance of pMUT-based communication links and, at the same time, enable pMUTs' frequency reconfigurability. By using a high-quality factor (Q) MEMS resonator as matching network (MN), we show that a substantial increase in a pMUTbased underwater receiver (Rx) sensitivity can be achieved at the cost of a reduced bandwidth. The out-of-band boosted response is significantly higher than what is achieved by the standalone pMUTs sensitivity. This means that the system peak sensitivity is set by the MN resonance, and it is independent from the pMUTs center frequency. Therefore, we show that by multiplexing different MNs it is possible to reconfigure pMUTs' operation. Moreover, we demonstrate that, by loading the MEMS resonator MN (MRMN) with different commercial off-the-shelf (COTS) resistors, we can tune the trade-off between sensitivity and bandwidth (BW).

Index Terms—MEMS, pMUTs, reconfigurable, IoT

I. INTRODUCTION

THE development of the Internet of Things (IoT) envisions distributed communication networks relying on wireless, self-powered sensing nodes [1]. In this framework, piezoelectric Micromachined Ultrasound Transducers (pMUTs) come naturally into play for ultrasound-based communication given their small footprint and excellent performance in air [2], water [3], and intra-body [4] applications. This class of devices can count on limited fabrication complexity and design flexibility in selecting their operating frequency (f_s) [5]. Nevertheless, while pMUTs can be designed to operate in a frequency range as wide as 20 kHz to 20 MHz, once the devices are fabricated their sensitivity spectral response is fixed, as it depends on the devices' geometrical dimensions, such as the piezoelectric layer thickness and the membrane diameter [5].

In this work, we leverage the recent demonstration of pMUTs Matching Network (MN) boosting [6] to enable their reconfigurability. By employing a high Q MEMS resonator as MN, we show our system's Receiver (Rx) capability of transducing incident ultrasound waves with high sensitivity at frequencies that are well outside the natural bandwidth of the pMUT, and that are only set by the frequency response of the MEMS resonator MN (MRMN). Therefore, by multiplexing different MRMNs, we are able to reconfigure the Rx operating frequency.

Moreover, we explore an additional degree of reconfigurability at a fixed frequency by loading the MRMN with different commercial off-the-shelf (COTS) resistors, trading off passive amplification for larger bandwidth (BW), and providing a further degree of freedom to the IoT node designer.

To demonstrate the concept, 36% Sc-doped Aluminum Nitride (ScAlN) 20x20 pMUT arrays were employed. Such relatively new material has been demonstrated to increase AlN piezoelectric coefficients [7], allowing the fabrication of pMUTs with improved [8] and new [9] performance.

Section II presents an overview of the boosted Transmitter (Tx) and Rx, while section III showcases an experimental demonstration of the pMUTs reconfigurability, including the gain-BW trade-off.

II. BOOSTED TX AND RX

An electrical model of the MRMN-boosted Tx and Rx is depicted in Fig. 1a. The pMUT (Fig. 1b) dynamics is represented by an RLC circuit (R_m , L_m , and C_m) that describes the device's behavior in the mechanical domain (motional branch) and by a static capacitance (C_0) in the electrical domain. The transduction from one domain to the other is carried out by a transformer of ratio set by the transduction coefficient η . The Tx and Rx models differ in how the MRMN is interfaced with the PMUT: it is connected in series to the pMUT (or pMUT array) in the Tx, and in parallel to it in the Rx.

A. Boosted Tx

In an ultrasound Tx, an input electrical signal is converted into acoustic waves which are radiated into the surrounding medium, which is described in the equivalent circuit by the radiation impedance Z_M in the mechanical domain. Due to the relatively poor electromechanical coupling (k_t^2) of flexural resonators (typically < 1%) most of the electrical energy provided to the system flows in to the electrical capacitance C_0 . While the more energy flows into the mechanical branch at the natural resonance of the pMUT plate, the limited quality factor of flexural resonators (especially in water) provides limited increase in sensitivity. In a resonator-boosted Tx (bTx), instead, given an MRMN of resonance frequency f_{sMN} , the MEMS resonator acts as a high-Q inductor resonating out the static capacitance of the pMUT (connected in series) at a frequency close to f_{sMN} , in a similar mechanism as the one described in [10]. In this way, a voltage build-up across C_0 is possible, charging the pMUTs electrical capacitance with a time constant that is proportional to the MN quality factor. This mechanism allows the bTx to generate more acoustic pressure than a conventional Tx per unit input voltage, or alternatively to transmit at across the same range with a lower amplitude input signal. Since the quality factor of the pMUT is typically very

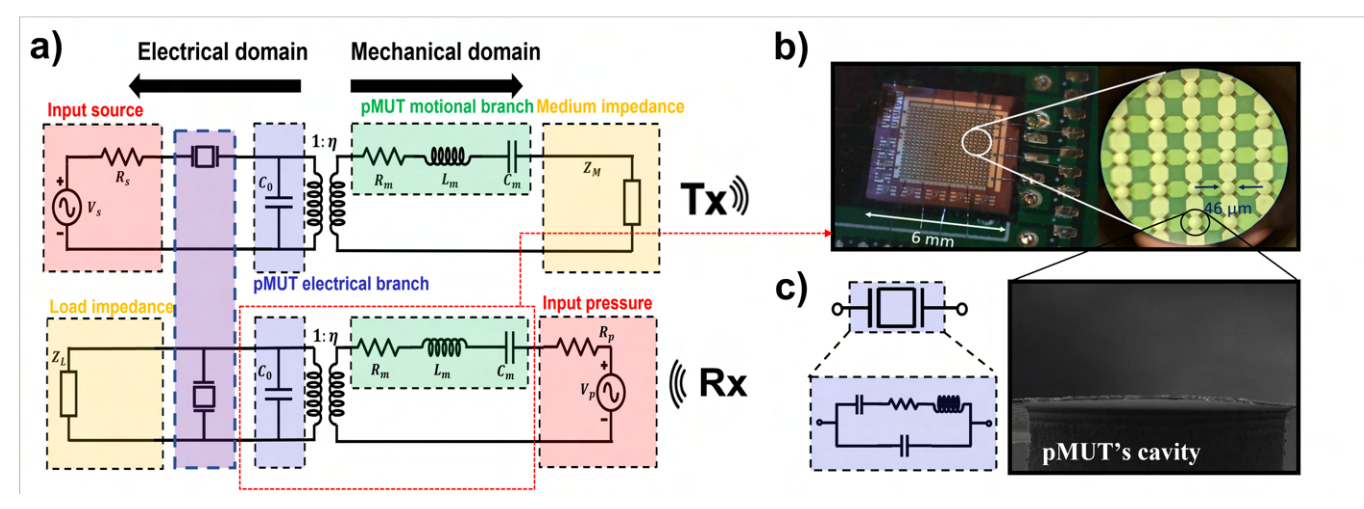


Fig. 1. a) Boosted Tx and Rx schematics, depicting the electrical equivalent circuit of the pMUT and highlighting the systems' symmetry (except for the MN element), b) micrograph of the bonded pMUT array employed in this work with a Scanning Electron Microscope (SEM) zoom-in to a device's cross-section showing the membrane and the cavity. In c), the Butterworth-Van Dike model of a piezo-MEMS resonator is shown.

low, we note that the transmission improvement is not affected by the pMUTs natural frequency, and is mainly determined by the center frequency of the MRMN.

B. Boosted Rx

In a pMUT-based Rx, incoming ultrasound sets the transducer in motion, which converts the sound wave into an electrical signal to be delivered to its load (Z_L) . In a resonator-boosted Rx (bRx), to maximize the voltage build-up across the pMUT electrodes, the MN is connected in parallel to the transducer. When the MRMN operates in it inductive region, it acts as a high-Q inductor generating a parallel resonant circuit with the static capacitance. In this way, a high impedance node is created, allowing much more current to flow into the Rx's load, thus increasing the system's sensitivity. As for the bTx case, the increase in sensitivity generated by the introduction of MRMN is not tied to the position of the natural frequency of the pMUT, but it is rather set by the antiresonance frequency of the MRMN. Frequency reconfigurability can therefore be achieved by multiplexing multiple resonators to the same pMUT array.

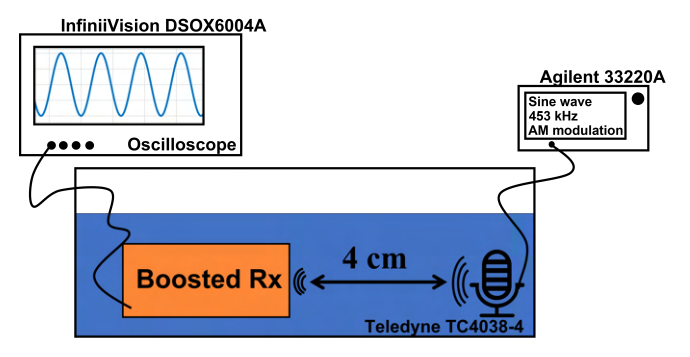


Fig. 2. Visual representation of the employed underwater experimental setup. It includes the water basin, the boosted Rx, the COTS hydrophone used as broadband Tx, the signal generator, and the oscilloscope.

III. EXPERIMENTAL RESULTS

The experiments presented in this work have been performed on a bRx constituted by a 36% Sc-doped Aluminum Nitride (ScAlN) 20x20 pMUT array. The devices were fabricated with the same procedure described in [6], while the piezo-film was sputtered as in [11]. COTS MEMS resonators and resistors were used as MRMNs. The natural frequency of the PMUTs in the array was measured at 700 kHz in water. Fig. 2 shows the underwater testing setup. As shown, the bRx was submerged in water, while a COTS hydrophone (Teledyne TC4038-4) was used as a Tx, emitting a broadband ultrasound spectrum. The Tx was connected to a signal generator (Agilent 33220A) and the bRx to an oscilloscope (Keysight DSOX6004A) in order to record the received signal.

A. pMUT's reconfigurability

To demonstrate pMUT's reconfigurability, two different MRMNs were selected (R1 and R2), with anti-resonance frequencies $f_{p1} = 460.1$ kHz and $f_{p2} = 445.9$ kHz, respectively. A sine wave at $f_{in} = 453$ kHz sine-modulated at $f_{mod} = 7.1$ kHz and was then applied to the Tx, generating the received Fourier spectrum shown in Fig. 3a in absence of the MRMN. As it can be observed, there are 3 peaks, at $f = f_{in}$ and at $f = \pm f_{mod}$, with the peaks standing at approximately the same (low) amplitude given that the 3 frequencies are outside of the pMUTs' 700 kHz natural frequency band. When connecting R1, the spectral response changes to the one of Fig. 3b, with more than 20 dB voltage gain for the frequency $f_{in} + f_{mod}$ with respect to the un-boosted case. A similar behavior is observed when connecting the second MRMN (Fig. 3c), also boosting the spectral response of $f_{in} - f_{mod}$ by more than 20 dB.

This experiment demonstrates pMUTs' reconfigurability at the architectural level. Moreover, more MNs can be multiplexed, allowing the system to receive on multiple communication

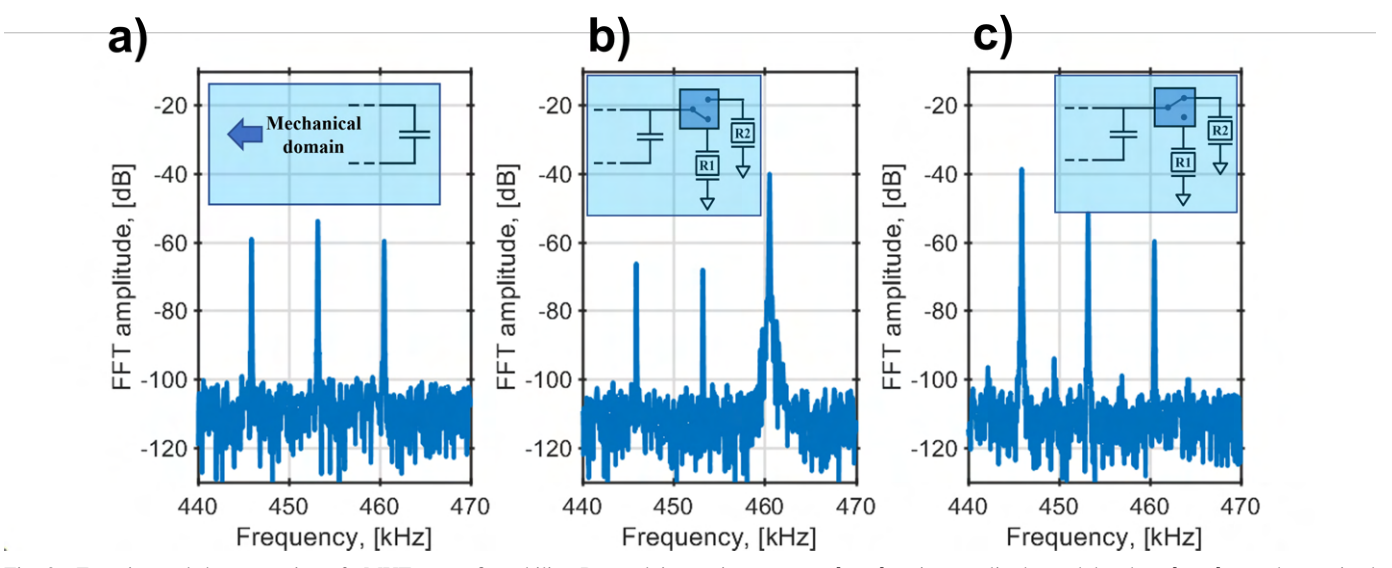


Fig. 3. Experimental demonstration of pMUTs reconfigurability. By applying a sine wave at $f=f_{in}$ sine-amplitude-modulated at $f=f_{mod}$, the received spectrum shows 3 peaks, at f_{in} and at $f_{in}\pm f_{mod}$. When applying the signal to a standalone pMUT array (a), the three peaks have low amplitude since the frequencies are out of band for the array. Nevertheless, when connecting the two MRMNs, one at a time, there is a significant (>20 dB) boost in the Rx sensitivity at a $f_{in}+f_{mod}$ (b) and $f_{in}-f_{mod}$ (c), respectively.

channels, one at a time, and benefiting from the increased sensitivity.

B. Gain-Bandwidth trade-off

The cost of using a high-Q MRMN to boost the PMUTs response is a narrowing of the system's band. The band decreases proportionally with the system's gain, and therefore with the MN's Q. Nevertheless, the quality factor of the resonator can be artificially reduced by loading it with COTS resistors, trading off the gain magnitude for the bRx's BW. This hypothesis was experimentally verified by connecting the pMUTs array to R1, and selecting different resistance values to load the MN, namely 0, 15, 47, 120, and 220 Ω . The bRx's normalized gain (G) vs. frequency is shown in Fig. 4a, along with the standalone array case. The gain in the case of no resistor, G = 11 corresponds to the 20.83 dB boost shown in Fig. 3b. Fig. 4b reports the obtained values of 3dB BW and normalized voltage gains as function of the loading resistor, and highlights their proportionality. Passing from a $0~\Omega$ load to a load of 220 Ω , the BW is increased by more than 6 times, while the gain is about 6 times smaller. Nevertheless, the bRx's sensitivity is still twice as much as a conventional un-boosted Rx at the same frequency.

These results demonstrate the second-order trade-off of the boosted systems, allowing a pMUT-based IoT front-end module with a switchable bank of resistors to adjust the BW (*i.e.* the communication data rate) as function of the distance with the node with which it is communicating, or as function of the required received signal to noise ratio.

IV. CONCLUSIONS

In this paper, the architectural-level MN-boosting concept introduced in [6] is extended from a way to increase pMUT-based transceivers performance to a more developed technique

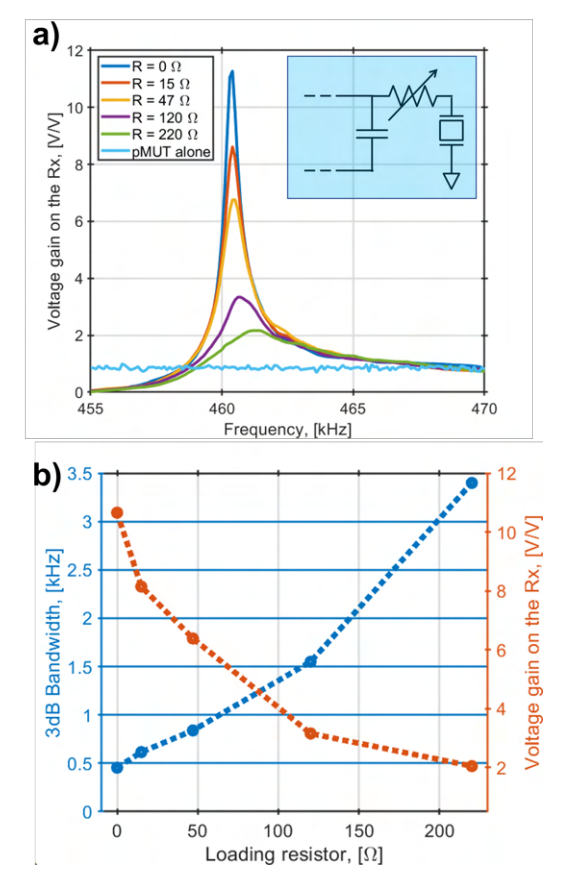


Fig. 4. a) Voltage gain on the bRx normalized to the case of the standalone pMUT as function of frequency for different loading resistors and b) gain and BW values for different loading resistors, highlighting the tradeoff.

with the purpose of enabling their frequency reconfigurability.

A circuital-level explanation of the MN-boosting mechanisms is provided, and its validity is verified through 2 sets of experiments involving a boosted Rx operating in underwater conditions. The experiments demonstrate three main points: 1) a significant 11x increase in sensitivity of an underwater Rx compared to a standalone pMUT one, 2) pMUTs frequency reconfigurability by connecting the array with a MEMS-resonator MN, and 3) the gain-BW trade-off, verified by loading the MN with a set of COTS resistors.

This demonstration points towards the realization of IoT node front-ends able to reconfigure their operation and adjust their data rate as function of the distance from the node(s) they are communicating with.

REFERENCES

- [1] S. C. Mukhopadhyay and N. K. Suryadevara, *Internet of Things: Challenges and Opportunities*, pp. 1–17. Cham: Springer International Publishing, 2014.
- [2] G.-L. Luo, Y. Kusano, and D. A. Horsley, "Airborne piezoelectric micromachined ultrasonic transducers for long-range detection," *Journal* of *Microelectromechanical Systems*, vol. 30, no. 1, pp. 81–89, 2021.
- [3] B. Herrera, F. Pop, C. Cassella, and M. Rinaldi, "Miniaturized pmut-based receiver for underwater acoustic networking," *Journal of Microelectrome-chanical Systems*, vol. 29, no. 5, pp. 832–838, 2020.
- [4] B. Herrera, G. Giribaldi, M. Pirro, L. Colombo, and M. Rinaldi, "Wireless ultrasonic power transfer for implantables via scandium-doped aln pmut arrays," in 2022 IEEE 35th International Conference on Micro Electro Mechanical Systems Conference (MEMS), pp. 837–840, 2022.

- [5] Y. Lu and D. A. Horsley, "Modeling, fabrication, and characterization of piezoelectric micromachined ultrasonic transducer arrays based on cavity soi wafers," *Journal of Microelectromechanical Systems*, vol. 24, no. 4, pp. 1142–1149, 2015.
- [6] G. Giribaldi, B. H. Soukup, P. Simeoni, L. Colombo, and M. Rinaldi, "Matching network-boosted 36% scaln pmut linear array," in 2022 IEEE 35th International Conference on Micro Electro Mechanical Systems Conference (MEMS), pp. 251–254, 2022.
- [7] M. A. Caro, S. Zhang, T. Riekkinen, M. Ylilammi, M. A. Moram, O. Lopez-Acevedo, J. Molarius, and T. Laurila, "Piezoelectric coefficients and spontaneous polarization of ScAlN," in *Journal of Physics: Condensed Matter*, vol. 27, May 2015.
- [8] Y. Kusano, I. Ishii, T. Kamiya, A. Teshigahara, G.-L. Luo, and D. A. Horsley, "High-spl air-coupled piezoelectric micromachined ultrasonic transducers based on 36% scaln thin-film," *IEEE Transactions on Ultrasonics, Ferroelectrics, and Frequency Control*, vol. 66, no. 9, pp. 1488–1496, 2019.
- [9] B. Herrera, M. Pirro, G. Giribaldi, L. Colombo, and M. Rinaldi, "Alsen programmable ferroelectric micromachined ultrasonic transducer (fmut)," in 2021 21st International Conference on Solid-State Sensors, Actuators and Microsystems (Transducers), pp. 38–41, 2021.
- [10] L. Colombo, A. Kochhar, G. Vidal-Álvarez, and G. Piazza, "High-figure-of-merit x-cut lithium niobate mems resonators operating around 50 mhz for large passive voltage amplification in radio frequency applications," *IEEE Transactions on Ultrasonics, Ferroelectrics, and Frequency Control*, vol. 67, no. 7, pp. 1392–1402, 2020.
- [11] G. Giribaldi, M. Pirro, B. H. Soukup, M. Assylbekova, L. Colombo, and M. Rinaldi, "Compensation of contact nature-dependent asymmetry in the leakage current of ferroelectric sexal1x n thin-film capacitors," in 2021 IEEE 34th International Conference on Micro Electro Mechanical Systems (MEMS), pp. 650–653, 2021.